**PRE-PRINT** of the article:
*Blocken B, Carmeliet J. 2008. Pedestrian wind conditions at outdoor platforms in a high-rise apartment building: generic sub-configuration validation, wind comfort assessment and uncertainty issues. Wind and Structures 11(1): 51-70.*

# Pedestrian wind conditions at outdoor platforms in a high-rise apartment building: generic sub-configuration validation, wind comfort assessment and uncertainty issues

B. BLOCKEN* and J. CARMELIET

*Building Physics and Systems, Technische Universiteit Eindhoven, P.O. box 513, 5600 MB Eindhoven, the Netherlands*

**ABSTRACT**

CFD is applied to evaluate pedestrian wind comfort at outdoor platforms in a high-rise apartment building. Model validation is focused on generic building sub-configurations that are obtained by decomposition of the actual complex building geometry. The comfort study is performed during the design stage, which allows structural design changes to be made for wind comfort improvement. Preliminary simulations are performed to determine the effect of different design modifications. A full wind comfort assessment study is conducted for the final design. Structural remedial measures for this building, aimed at reducing pressure short-circuiting, appear to be successful in bringing the discomfort probability estimates down to acceptable levels. Finally, the importance of one of the main sources of uncertainty in this type of wind comfort studies is illustrated. It is shown that the uncertainty about the terrain roughness classification can strongly influence the outcome of wind comfort studies and can lead to wrong decisions. This problem is present to the same extent in both wind tunnel and CFD wind comfort studies when applying the same particular procedure for terrain relation contributions as used in this paper.

## 1. Introduction

High-rise buildings can introduce high wind speed at pedestrian level, which can lead to uncomfortable or even dangerous conditions. Wind discomfort and wind danger can be detrimental to the success of new buildings. Wise (1970) reports about shops that are left untenanted because of the windy environment which discouraged shoppers. Lawson and Penwarden (1975) report the death of two old ladies due to an unfortunate fall caused by high wind speed at the base of a tall building. Today, many urban authorities only grant a building permit for a new high-rise building after a wind comfort study has indicated that the consequences for the pedestrian wind environment remain limited. Wind comfort studies can be performed using wind tunnels or numerical simulation with CFD.

Wind tunnel studies can use either point methods or area methods, or – preferably – a combination of both. Point methods (e.g. hot wire anemometry or laser Doppler anemometry) provide quantitative data at discrete locations in the flow field but are time-consuming if data at a large number of positions are to be obtained. Area methods such as scour techniques provide spatially continuous information but their use is mainly limited to providing qualitative, rather than quantitative information (Livesey et al. 1990). Particle Image Velocimetry (PIV) is an exception to this, but it suffers from other drawbacks such as laser sheet shielding, attenuation and reflections by the building models themselves. Ideally, area methods are used to determine the location of the wind comfort problem spots, followed by selected point measurements at these locations.

CFD studies for pedestrian wind comfort are most often based on the Reynolds-averaged Navier-Stokes (RANS) approach. Validation by comparison of the numerical results with experimental data is imperative. Most often, experimental data for the building configuration under study are not available. In such cases, another option for validation, as presented in this paper, is generic sub-configuration validation. It implies decomposition of the actual complex building geometry into simpler, generic building configurations, the flow around which exhibits similar features as the flow around the actual building configuration. Validation is then performed for the generic configurations, for which wind tunnel data are often available in the literature. If the numerical model

* **Corresponding author**: Bert Blocken, Building Physics and Systems, Technische Universiteit Eindhoven, P.O.Box 513, 5600 MB Eindhoven, the Netherlands. Tel.: +31 (0)40 247 2138, Fax +31 (0)40 243 8595
*E-mail address:* b.j.e.blocken@tue.nl

performs well for these configurations, it can reasonably be assumed that it will also provide reliable predictions for the more complex building configuration.

The new high-rise residential building project "Joan Miro" is part of the development of Genk, a city in the east of Flanders (Belgium). The design consists of a small group of (originally four) high-rise building blocks (26 m height) of nine floors each (Fig. 1a). At each floor, the buildings and their individual apartments are accessible by outdoor pedestrian platforms (Fig. 1b-c). These platforms connect the four blocks with each other and with the staircases and elevators. Concerns about possible wind comfort problems at the platforms led to the request to study the pedestrian wind environment and, if necessary, to provide remedial measures.

For this building, the application of both area and point wind tunnel measurement methods is complicated. Measurement data are needed at all outdoor platforms, but it is rather difficult to access these platforms in a model of the building with the sensor or laser beams because of the large number of enclosures surrounding these platforms, and because the configuration of the platforms is different at every floor. In this respect, CFD simulations provide some advantages. Because no experimental data are available, neither for this particular building configuration nor for very similar configurations, generic sub-configuration validation is applied.

Wind comfort studies imply assessment of exceedance probabilities of discomfort thresholds for a mean, gust or effective wind speed. A new standard for wind comfort, NEN8100, has recently been developed in the Netherlands (NEN 2006a, 2006b) based on research work by Willemsen and Wisse (2002, 2007), Wisse and Willemsen (2003), Verkaik (2006), Wisse et al. (2007), and others. The procedure used in this paper is to some extent different from the Dutch wind standard, because the building under study is located in Flanders, where not enough wind statistical data are available for the detailed assessment as outlined in NEN8100. This leads to additional uncertainties in the assessment procedure. Based on the outcome of the wind comfort study, remedial action may be necessary. For the present building, wind comfort assessment is performed in the early design stage and structural remedial measures, if needed, can be incorporated.

This paper presents the CFD evaluation of the pedestrian wind conditions at the outdoor platforms in the high-rise apartment building based on generic sub-configuration validation and a full wind comfort assessment study, followed by a discussion on some uncertainty issues. In section 2, the procedure for the assessment of wind comfort is briefly outlined. Section 3 contains a short description of the buildings, site and surrounding terrain. Model validation is performed in section 4. Section 5 consists of the suggestion and evaluation of different design modifications. In section 6, the wind comfort assessment study is provided. Finally, sections 7 (discussion) and 8 (conclusions) conclude the paper.

## 2. Procedure for the assessment of wind comfort

Three aspects are needed for wind comfort assessment: (1) statistical meteorological information; (2) aerodynamic information; and (3) a comfort criterion. The aerodynamic information is required to transfer the statistical meteorological information from the meteorological site to the point of interest at the building site. The transferred wind statistics are subsequently subjected to the wind comfort criterion.

### *2.1. Meteorological information*

The meteorological data should cover a period of several decades (typically 30 years) and should be exposure corrected. A number of meteorological institutes provide corrected data containing hourly mean values of potential wind speed ($U_{pot}$) and wind direction. $U_{pot}$ is the wind speed measured at 10 m height at an ideal meteorological station with an aerodynamic roughness length $y_{0,meteo}$ = 0.03 m.

### *2.2. Aerodynamic information*

The ratio of the local pedestrian-level mean wind speed $U$ at the location of interest to $U_{pot}$ is given by the total wind amplification factor $\gamma$, which can be split into contributions from different spatial scales: a design related contribution ($U/U_0$) or local amplification factor and a terrain related contribution ($U_0/U_{pot}$):

$$\gamma = \frac{U}{U_{pot}} = \frac{U}{U_0} \cdot \frac{U_0}{U_{pot}} \tag{1}$$

where $U_0$ is a reference wind speed that can be defined in various ways. In the wind comfort assessment study, it will be taken at pedestrian height ($y$ = 1.75 m) and at the location of the inlet of the computational domain. The local amplification factor $U/U_0$ can be determined by wind tunnel testing or by CFD. The terrain related contribution $U_0/U_{pot}$ takes into account the effect of the differences between the terrain roughness of the meteorological site and the roughness of the terrain upstream of the location of interest (city), as well as the difference in height between $U_0$ and $U_{pot}$. The Dutch standard NEN8100 allows a detailed and quite accurate assessment of terrain related contributions for any location in the Netherlands (Verkaik 2006, Willemsen and

Wisse 2007). Because such information is not available for Flanders, an alternative, more traditional, but also less accurate approach has to be adopted. The terrain related contribution is estimated using the logarithmic law for both terrain types:

$$\frac{U_0}{U_{pot}} = \frac{U_{city}(y=1.75\,m)}{U_{meteo}(y=10\,m)} = \frac{u^*_{city}\cdot\ln\left(\frac{1.75\,m}{y_{0,city}}+1\right)}{u^*_{meteo}\cdot\ln\left(\frac{10\,m}{y_{0,meteo}}+1\right)} \quad (2)$$

where $y$ is the height coordinate and $u^*$ is the friction velocity. The relation between $u^*_{city}$ and $u^*_{meteo}$ is given by Simiu and Scanlan (1986):

$$\frac{u^*_{city}}{u^*_{meteo}} = \left(\frac{y_{0,city}}{y_{0,meteo}}\right)^{0.0706} \quad (3)$$

Following this procedure, values for the conversion factor $\gamma_\theta$ are obtained for each wind direction $\theta$. Some implications of this approach on the uncertainty of the predicted discomfort probabilities will be discussed later in this paper.

### *2.3. Comfort criterion*

Many wind comfort criteria have been suggested and used in the past. A comparison of about 30 criteria was made by Bottema (2000). Large and sometimes very large differences were found between criteria, most likely due to the fact that most criteria were based on intuition rather than on experimental surveys. In the code NEN8100, the threshold value for the mean wind speed is 5 m/s for all grades of wind comfort and 15 m/s for wind danger. Note that only mean wind speed is considered in the threshold value, while gustiness is not. The criteria for wind comfort and wind danger are given in Table 1. They are based on the small amount of experimental information available in the literature and on the established practice and experience in the Netherlands. More detailed information on the selection of these criteria can be found in Willemsen and Wisse (2007).

### *2.4. Relationship between total wind amplification factor and discomfort probability*

For a given discomfort threshold $U_{THR}$ and given wind statistics, the relationship between $\gamma_\theta$ and the discomfort probability $P_\theta$ for each wind direction $\theta$ can be established. It is based on the combination of the Weibull distribution function and the total wind amplification factor (see e.g. Blocken et al. 2004):

$$P_\theta(U > U_{THR}) = 100\cdot A(\theta)\exp\left[-\left(\frac{U_{THR}}{\gamma_\theta\cdot c(\theta)}\right)^{k(\theta)}\right] \quad (4)$$

where $P_\theta(U > U_{THR})$ is the probability of exceedance of $U_{THR}$ = 5 m/s by the local wind speed $U$ during wind direction $\theta$ and $A(\theta)$, $c(\theta)$ and $k(\theta)$ are the Weibull parameters, respectively denoting: probability for wind direction $\theta$, velocity scale for wind direction $\theta$ (m/s), shape parameter for wind direction $\theta$. The Weibull parameters are determined by fitting the Weibull distribution function to the statistical meteorological data. Calculating and summing $P_\theta$ for all wind directions yields the total discomfort probability $P$ to be compared with the values in Table 1.

## 3. Description of building, site and terrain

The building configuration (original design) is illustrated in Fig. 1a-c. The dimensions of the building, including the four blocks A-D and the passages between them, are $L$x$D$x$H$=61x22x26 m³. All blocks have nine floors and are connected by outdoor pedestrian platforms. The configuration of the platforms is different at each floor. The building is situated in the city centre as illustrated in Fig. 2 and 3. Genk is a city with only a limited number of high-rise buildings. Most of them are situated in the city centre: flats alongside the planned apartment building and a few high-rise buildings at the east side of the centre (as indicated in Fig. 2). Outside the centre, the city consists of concentrations of mainly low-rise buildings (not shown in the figures). The aerodynamic roughness length of the surrounding terrain (for a distance of up to 5 to 10 km) is estimated from the knowledge of the surroundings, from the corresponding topographic map and from the updated Davenport roughness classification

(Wieringa 1992). No large differences are observed for the different wind directions, and $y_0$ = 0.5 m is selected for all 12 wind direction sectors.

## 4. Model validation

### *4.1. Decomposition into generic sub-configurations*

From a wind flow point of view, the original design (Fig. 1a-c) can be decomposed into three sub-configurations (Fig. 4): (1) a passage between two parallel buildings, placed side-by-side (Fig. 4a; Type-1 flow); (2) a passage through a building (Fig. 4b; Type-2 flow); and (3) a passage between two parallel buildings that are shifted towards each other (Fig. 4c; Type-3 flow). Type-1 flow occurs between building blocks A and C, between A and B, between B and D and between C and D (see Fig. 1c). But, with the presence of the pedestrian platforms at all levels, closing to some extent the passages at the bottom and top, this flow type might also exhibit features of Type-2 flow. Type-3 flow is present between blocks B and C. In all three configurations the main reason for high wind speed and possible wind comfort problems in the passages is "pressure short-circuiting", which occurs because the passage connects the windward (overpressure) and leeward (underpressure) facade of the building(s) (Fig. 5).

Validation for Type-1 flow and Type-2 flow has been conducted to some extent in previous papers (Blocken et al. 2004, Blocken et al. 2007a) based on wind tunnel measurements by Stathopoulos and Storms (1986) and Wiren (1975) and will not be repeated here. Passages between parallel buildings shifted from each other (Type-3 flow) are considered the most important generic sub-configuration for the present study. This validation study is reported in this paper.

### *4.2. Experimental data*

Wind tunnel data for wind flow in passages between generic parallel shifted buildings are rather scarce. Beranek (1982) provided some sand erosion test results for shifted buildings, the geometry of which is roughly similar to that of building blocks B and C (Fig. 1c). It has been noted that sand erosion tests are considered somewhat less suitable to obtain quantitative results and that their use should rather be limited to qualitative comparisons (Livesey et al. 1990). The reason is that the results from sand erosion experiments can be quite variable depending on parameters such as the shape and size distribution of the sand particles used, the length of the time intervals during which erosion is allowed to occur and the fact that sand erosion is not a localised phenomenon, since sand particles eroded at a certain location will impact further downstream and can also erode particles at these other locations, even if the local wind speed forces at those locations are not large enough to erode particles by themselves. Quantitatively more reliable data has been made available in the CEDVAL database (Leitl 2000). Although the latter data should normally be preferred, the geometry of the building configurations in those tests is quite different from that of blocks B and C. Therefore, in spite of a somewhat reduced validation capacity, Beranek's data are selected for this study.

The experiments by Beranek (1982) were performed at a scale of 1:500 with a power law wind speed profile with exponent $\alpha$ = 0.28. Fig. 6a (left column) displays sand erosion contour plots that provide a measure of the amplification factor $U/U_0$, i.e. the ratio of the local wind speed and the wind speed that would exist at the same location if the buildings were absent. The building dimensions are indicated in the figure, where s is the distance (perpendicular) between the buildings. Very high amplification factors are found in the passages between the buildings. Note that Fig. 6(a3) is not a shifted building configuration but, due to the orientation of the building group, the same pressure short-circuiting effect governs the flow in these passages.

### *4.3. Simulation characteristics and settings*

The dimensions of the computational domain are chosen to limit the maximum blockage ratio to 3.6%. The aim of the model validation is to provide confidence for the CFD simulations for the rather complex apartment building. Because of the complexity of that building geometry, an unstructured grid with tetrahedral cells will be used. Therefore, a similar grid has to be used in the validation study. The grids for model validation are obtained based on grid-sensitivity analyses and their size is in the range of $0.7 \times 10^6$ to $1.5 \times 10^6$ cells, depending on the building geometry. A relatively large amount of cells is needed to obtain a "grid-independent solution" because many cells are required in the rather long and wide passages.

The CFD simulations are conducted with the commercial code Fluent 6.2 and the 3D RANS equations. Closure is provided by the realizable k-ε model (Shih et al. 1995). The governing equations are solved using the control volume method. Pressure-velocity coupling is taken care of by the SIMPLE algorithm. Pressure interpolation is second order. Second order discretisation schemes are used for both the convection terms and the viscous terms of the governing equations.

The inlet mean wind speed profile is taken equal to the measured wind tunnel profile. Turbulent kinetic energy and turbulence dissipation rate are given by Eq. (5) and (6) (Richards and Hoxey 1993):

$$k(y) = \frac{(u^*)^2}{\sqrt{C_\mu}} \quad (5)$$

$$\varepsilon(y) = \frac{(u^*)^3}{\kappa(y + y_0)} \quad (6)$$

where $y$ is the height co-ordinate, $C_\mu$ is a constant (0.09) and $\kappa$ the von Karman constant (~ 0.42). The friction velocity u* is determined by fitting the log law to the power law with $\alpha = 0.28$. The sides and the top of the computational domain are modelled as slip walls (zero normal velocity and zero normal gradients of all variables). At the outlet, zero static pressure is specified. The non-equilibrium wall functions by Kim and Choudhury (1995) with equivalent sand-grain roughness ($k_S$) modifications according to the formulae by Cebeci and Bradshaw (1977) are used. The use of such $k_S$-type wall functions can yield difficulties in simulating a horizontally homogeneous ABL, which is often required in the upstream part of computational domains (Blocken et al. 2007b). Horizontal homogeneity refers to the absence of streamwise gradients in the vertical profiles of mean wind speed and turbulence quantities in the region that is not disturbed by the presence of building models (Richards and Hoxey 1993, Blocken et al. 2007a, 2007b). For CFD simulations of a horizontally homogeneous ABL with $k_S$-type wall functions, the appropriate relationship between $k_S$, $y_0$ and the roughness constant $C_S$ should be satisfied. This relationship was derived for Fluent 6.2 and for Ansys CFX 10.0 in an earlier paper by the authors (Blocken et al. 2007b). For Fluent 6.2, this relationship is:

$$k_S = \frac{9.793\ y_0}{C_S} \quad (7)$$

Note that Fluent 6.2 does not allow $k_S$ to be larger than $y_P$, which is the distance between the centre point of the wall-adjacent cell and the wall. If the user implements a larger value, the code will automatically set $k_S$ equal to $y_P$ without warning. Therefore, in this study, $k_S$ is taken equal to $y_P$ (0.2 m) and $C_S$ is chosen to satisfy Eq. (7). A user-defined function setting the value of the constant $C_S$ is required because the code does not allow exceeding the interval [0;1] otherwise. The occurrence of unintended streamwise gradients with these settings is tested in an empty computational domain with a similar grid distribution as the actual domain. A good horizontal homogeneity of the vertical mean wind speed, turbulent kinetic energy and turbulence dissipation rate profiles is observed.

### *4.4. Simulation results and validation*

Fig. 6b displays the numerical results in terms of $U/U_0$ in a horizontal plane at a height of 2 m above ground. Note that just part of the bottom of the computational domain is shown in the figure. Comparing Figs. 6a and 6b shows a good qualitative agreement and even a good quantitative agreement, at least where the highest amplification factors are concerned:

1. The regions with high and low $U/U_0$ are similar in the numerical and in the experimental results: (a) Figs. 6(a1-b3): the high wind speed regions in the passages and the corner streams; (b) Figs. 6(a1-b3): the stagnation regions in front of the buildings; (c) Figs. 6(a1-b1): the standing vortices in front of the buildings.
2. The magnitude of the numerical and the experimental $U/U_0$ in the passages, in the corner streams and in the standing vortices are generally in good agreement.

However, there are also a number of discrepancies:

1. The values of the lower $U/U_0$ found by numerical simulation are significantly smaller than those from the experiments.
2. In Fig. 6(b2), the numerical results yield a larger $U/U_0$ than the experiments in the passage to the right.

This can, apart from turbulence model limitations, at least partly be attributed to the fact that $U/U_0$ in the experimental study results from a comparison of the sand erosion process at different wind speed values, while in the numerical study it is a direct ratio of wind speed values. In the experimentals, turbulent fluctuations can be an important factor in the removal of the sand particles, while in the calculations only mean wind speed values are used to obtain $U/U_0$. Nevertheless, the present validation of the CFD model provides some confidence that wind conditions in passages between shifted buildings can be modelled numerically with satisfactory accuracy, at least where the highest values of $U/U_0$ are concerned.

## 5. Evaluation of design modifications

Significant wind comfort problems due to pressure short-circuiting are anticipated in all passages between the individual building blocks (Fig. 1c and 7a). The design modifications are straightforward and are aimed at eliminating pressure short-circuiting. In a first step, the narrow passages between the building blocks are closed (Fig. 7b). In a second step, the remaining passage between the two L-shaped blocks is closed by insertion of a central staircase (Fig. 7c). The original situation and the effect of the design modifications are evaluated by CFD simulations for three simplified models. Because these simulations are only intended to evaluate the overall effect of the design changes, the surroundings buildings, the platforms and other building details are not yet included in the models. A power law exponent of 0.28 (~ $y_0$ = 0.5 m) is used for the velocity inlet. The inlet turbulence profiles are given by Eqs. (5) and (6). The blockage ratio for each model is 2.6%. The unstructured tetrahedral grids comprise $1.8 \times 10^6$, $8.0 \times 10^5$ and $8.0 \times 10^5$ control volumes respectively. The large number of control volumes for the first model (first design) was needed to accurately model the wind flow in the narrow passages between building blocks A and B and between C and D. The 3D calculations are made with the commercial CFD code Fluent 6.2, and all other simulation characteristics and settings are as in section 4.3.

Figs. 8a-c illustrate the results in terms of pedestrian-level $U/U_0$. Note that the white spots in the corner streams that are surrounded by black filled contours indicate that $U/U_0$ locally exceeds the value of 2.0. Especially the third design modification provides a large improvement of the wind conditions. Fig. 9 shows $U/U_0$ roses for the three designs, giving the maximum value in the passage for each of the 12 wind directions, indicating the same significant improvement. Note that for the first design, $U/U_0$ was taken in the main west-east oriented passage, not in the narrow passages where sometimes higher values were found.

## 6. Wind comfort assessment for the final design

The wind comfort assessment study is performed on a computational model of Genk city centre (Fig. 2 and 3). While the geometry of the apartment itself is modeled in detail, the buildings in the immediate vicinity of the residence are only included with their main shape (see Fig. 2 and 3: city hall, administration department, flats alongside apartment building, low-rise and medium-rise buildings between streets “Dieplaan” and “Grotestraat”). Buildings at a larger distance from the apartment building that are expected to have a lesser influence on the wind flow around and through it are only roughly modelled together with the terrain elevations as large volumes (see Fig. 2 and 3: concentrations of high-rise, medium-rise and low-rise buildings) with increased roughness characteristics: $y_0$ = 0.5 m, $C_S$ according to Eq. (7). The model is immersed in an atmospheric boundary layer with a logarithmic mean velocity inflow profile corresponding to the estimated roughness length ($y_0$ = 0.5 m). The inlet turbulence profiles are given by Eqs. (5) and (6). The computational domain has dimensions $L_D \times B_D \times H_D$ = 1500x1000x100m³. The blockage ratio is about 3%. An unstructured, tetrahedral grid with about $3.0 * 10^6$ cells is used. The grid on the surface of the apartment building and on some of the surrounding buildings is depicted in Fig. 10a. Note that, while the grid resolution is rather low on the surfaces of the surrounding buildings, the resolution is quite high near the details of the residence itself. At these locations, at least 10 cells were provided along the length, width and height of every geometrical detail (Franke et al. 2007). Other simulation characteristics are identical to those in section 4.3. The steady-state wind flow pattern is calculated for 12 wind directions. As an example, the calculation results for north wind direction at the fifth floor are given in Fig. 10b. Contours of $U/U_0$ are shown, where $U$ is the local mean wind speed at 1.75 m above the fifth floor (pedestrian height) and $U_0$ is the reference mean wind speed at 1.75 m height at the inlet of the computational domain. High values up to 1.3 occur near the platform in the north-facing cavity. Also at higher floors and in the other cavity, high values can occur, up to 2.3 at the eight floor, which are due to the vertical flow in the cavity caused by pressure short-circuiting between the lower and the upper part of the cavity. The staggered arrangement of the platforms at each floor allows the wind to sweep vertically between them (Fig. 11).

The meteorological data (30-year hourly potential wind speed and wind direction) from Eindhoven are used, because of lack of such data in Flanders and because of the proximity of Genk to Eindhoven (80 km over relatively flat terrain). The complete procedure for wind comfort assessment, as outlined in section 2, yields the exceedance probabilities $P$ in Fig. 12 (bars for $y_0$ = 0.5 m). A distinction is made between two cavities, as generated by the addition of the central staircase in Fig. 7c. N and S refer to the cavities facing north and south, respectively. As such, N5 refers to the north-facing cavity at the fifth floor. Note that for all floors and for each cavity, the amplification factors at the worst positions are always considered in calculating $P$. The $P$ values for the ground floor and the first four floors are all equal to zero and the values at the higher floors – except for S8 – are less than 10%, indicating a good wind comfort for traversing (see Table 1). For position S8, wind comfort is moderate. A wind danger assessment shows that the danger probabilities at all floors are zero. Overall, wind comfort can be judged to be favourable, at least if the applied procedure can be considered accurate enough,

which will be discussed in the next section. Regardless, comparing the local amplification factors for the three different designs in Figs. 8 and 9, it is clear that the original design would have suffered from serious wind comfort problems.

Concerning the final design, it is important to note that special attention has to be paid regarding the doors in the central staircase, because simultaneously opening opposite doors of the staircase will give rise to pressure short-circuiting. This will lead to sudden and hence surprising wind gusts through the staircase which must be avoided.

## 7. Discussion

In the past, wind tunnel testing has been the primary tool to determine design related contributions ($U/U_0$) in wind comfort studies. Currently, CFD is also becoming increasingly recognised as a valuable tool for pedestrian wind comfort studies in complex urban environments (ASCE 2003). As an example, NEN (2006a) explicitly offers CFD as an alternative for wind tunnel studies, provided that a list of demands for quality assurance is satisfied. Several wind comfort studies in the past were performed with CFD (e.g. Richards et al. 2002, Hirsch et al. 2002, Blocken et al. 2004). The use of CFD has received significant support from the recent multitude of research efforts focused on improving the quality of CFD simulations for pedestrian wind studies, including the CFD guidelines by Franke et al. (2004), updated in 2007 (Franke et al. 2007) and those by the Architectural Institute of Japan (Mochida et al. 2006, Yoshie et al. 2007). Also many other research efforts have focused on the improving the quality of CFD simulations, such as those concerning the simulation of equilibrium atmospheric boundary layers in computational domains (e.g. Richards et al. 2002, Franke and Frank 2005, Blocken et al. 2007a, 2007b, Hargreaves and Wright 2007, Yang et al. 2007).

Although CFD will not be able to replace the wind tunnel in the foreseeable future (Stathopoulos 2002), its use in combination with wind tunnel studies provides opportunities. In the present study, wind tunnel measurements at the enclosed outdoor platforms in the apartment building model would have been rather difficult. CFD is a valuable alternative, although the support by generic sub-configuration validation based on available wind tunnel data is considered a minimum requirement.

The numerical simulations of the wind flow pattern and the procedure for wind comfort assessment introduce a number of errors and uncertainties. Efforts have been made to reduce these by: (1) the validation study for the three generic sub-configurations; (2) systematic grid sensitivity analyses; and (3) the use of the criteria in NEN8100 that take into account to some extent the errors made in the calculation of the discomfort probabilities (Willemsen and Wisse 2002, 2007). A particular source of uncertainty in the wind comfort assessment procedure, for which no specific precautions were taken, is the transformation of the wind statistics by means of the terrain related contribution $U_0/U_{pot}$ (Eqs. 2 and 3). While considerable effort is devoted to determining the design related contribution $U/U_0$, much less care is given to the terrain related contribution. Both the estimation of the aerodynamic roughness length $y_{0,city}$ from the roughness classification and the simplifications embedded in Eqs. (2) and (3) are prone to error. Note that this is a problem for both wind tunnel and CFD wind comfort studies. For example, it is not that difficult to be one class off in estimating the terrain roughness $y_{0,city}$ in the updated Davenport roughness classification (Wieringa 1992), which in this case could result in an $y_{0,city}$ of 0.25 m or 1 m instead of 0.5 m. To illustrate the consequences of this uncertainty, discomfort probabilities have also been determined with these $y_{0,city}$-estimates. Fig. 12 illustrates the large sensitivity of the discomfort probability $P$ to $y_{0,city}$, and shows that for $y_{0,city}$ = 0.25 m, wind comfort at S8 is poor. The reason for this large influence of $y_{0,city}$ on $P$ is the logarithmic function in the nominator of Eq. (2). Fig. 13a indeed shows the strong variation of $U_0/U_{pot}$ with $y_{0,city}$. As a general example, Fig. 13b shows the large sensitivity of the total discomfort probability $P$ to $y_{0,city}$, with the local amplification factor $U/U_0$ as a parameter. Note that the curves in Fig. 13b do not apply exactly to the case study in this paper, because Fig. 13b is constructed assuming that $U/U_0$ is the same for all wind directions, while Fig. 9 indicates that this is not completely true. Considerable effort has been made in NEN8100 to provide improved roughness mapping (Verkaik 2006) to assist in wind comfort studies, which has resulted in a new practice guideline and software to determine the mean hourly wind speed statistics at any location in the Netherlands (NEN 2006a). Such detailed information however is not available for Flanders and many other regions and countries, and could therefore not be applied in the present study. This can compromise the results of such studies, and lead to wrong decisions, for example at position S8 in this case. Future wind comfort studies would greatly benefit from the availability of detailed roughness mapping data in other countries.

## 8. Conclusions

CFD has been applied to evaluate pedestrian wind comfort at outdoor platforms in a high-rise apartment building. Model validation has focused on generic building configurations that are obtained by decomposition of the actual complex building geometry. This methodology of generic sub-configuration validation evidently does not provide full confidence, but, in absence of wind tunnel measurements for the actual geometry or for very similar complex geometries, it is often the only option.

The main reason for high wind speed in the original building design was pressure short-circuiting between the windward and leeward building facade. The most logical and straightforward solution was closing the narrow passages and placing an obstruction in the main passage. Wind amplification factors above unity still remain at some locations in the cavities, up to 2.3 at the eight floor, due to vertical pressure short-circuiting between the lower and the upper part of the cavity, and the staggered arrangement of the platforms that allows the wind to sweep vertically between them. In spite of this effect, the wind comfort in the modified building design can be judged favourable, at least if the applied procedure can be considered accurate enough.

An important source of uncertainty in the wind comfort assessment procedure, as outlined in this paper, is the calculation of the terrain related contribution of the total wind amplification factor. In particular, the resulting discomfort probabilities can be very sensitive to the value of the upstream aerodynamic roughness length, which is estimated from a roughness classification. This might change the outcome of such studies and lead to wrong decisions. This problem is present in both wind tunnel and CFD wind comfort studies. Improved roughness mapping is required for increased accuracy.


## Acknowledgements

The authors are grateful to Wendy Desadeleer for her kind assistance in the preparation of this paper. The Royal Dutch Meteorological Institute is acknowledged for providing the meteorological data used in this research.


## References


ASCE Aerodynamics Committee (2003), *Outdoor human comfort and its assessment*, State of the Art Report, Task Committee on Outdoor Human Comfort, American Society of Civil Engineers, Boston, VA, USA.

Beranek, W.J. (1982), *On avoiding wind nuisance around buildings, part 2 (Beperken van windhinder om gebouwen, deel 2)*, (in Dutch) Stichting Bouwresearch no. 90, Kluwer Technische Boeken BV, Deventer.

Blocken, B., Roels, S. and Carmeliet, J. (2004), "Modification of pedestrian wind comfort in the Silvertop Tower passages by an automatic control system", *J. Wind Eng. Ind. Aerodyn.*, **92**(10), 849-873.

Blocken. B., Carmeliet, J., and Stathopoulos, T. (2007a), "CFD evaluation of the wind speed conditions in passages between buildings – effect of wall-function roughness modifications on the atmospheric boundary layer flow", *J. Wind Eng. Ind. Aerodyn.*, **95**(9-11), 941-962.

Blocken, B., Stathopoulos, T., and Carmeliet, J. (2007b), "CFD simulation of the atmospheric boundary layer: wall function problems", *Atmos. Environ.*, **41**(2), 238-252.

Bottema, M. (2000), "A method for optimisation of wind discomfort criteria", *Build. Environ.*, **35**, 1-18.

Cebeci, T. and Bradshaw, P. (1977), *Momentum transfer in boundary layers*, Hemisphere Publishing Corporation, New York.

Franke, J., Hirsch, C., Jensen, A.G., Krüs, H.W., Schatzmann, M., Westbury, P.S., Miles, S.D., Wisse, J.A. and Wright, N.G. (2004), "Recommendations on the use of CFD in wind engineering", *International Conference on Urban Wind Engineering and Building Aerodynamics*, COST Action C14, Impact of Wind and Storm on City Life Built Environment, von Karman Institute, Sint-Genesius-Rode, Belgium.

Franke, J. and Frank, W. (2005), "Numerical simulation of the flow across an asymmetric street intersection", *Proceedings of the 4th European and African Conference on Wind Engineering (4EACWE)*, Prague, Czech Republic.

Franke, J., Hellsten, A., Schlünzen, H. and Carissimo, B. (2007), "Best practice guideline for the CFD simulation of flows in the urban environment". COST Action 732: Quality Assurance and Improvement of Microscale Meteorological Models.

Hargreaves D.M. and Wright, N.G. (2007), "On the use of the k–ε model in commercial CFD software to model the neutral atmospheric boundary layer", *J. Wind Eng. Ind. Aerodyn.*, **95**(5), 355-369.

Hirsch, C., Bouffioux, V. and Wilquem, F. (2002), "CFD simulation of the impact of new buildings on wind comfort in an urban area", *Workshop Proceedings, Cost Action C14, Impact of Wind and Storm on City Life and Built Environment*, Nantes, France.

Kim, S-E. and Choudhury, D. (1995), "A near-wall treatment using wall functions sensitized to pressure gradient", *ASME FED Vol. 217, Separated and Complex flows.*.
Lawson, T.V. and Penwarden, A.D. (1975), "The effects of wind on people in the vicinity of buildings", *4th International Conference on Wind Effects on Buildings and Structures*, Heathrow.
Leitl, B. (2000), "Validation data for microscale dispersion modelling", *EUROTRAC newsletter* 22/2000.
Livesey, F., Inculet, D., Isyumov, N. and Davenport, A.G. (1990), "A scour technique for evaluation of pedestrian winds", *J. Wind Eng. Ind. Aerodyn.*, **36**, 779-789.
Mochida, A., Tominaga, Y., and Yoshie, R. (2006), "AIJ Guideline for Practical Applications of CFD to Wind Environment around Buildings", *4th International Symposium on Computational Wind Engineering (CWE2006)*, Yokohama, Japan.
NEN. (2006a), *Wind comfort and wind danger in the built environment,* NEN 8100 (in Dutch) Dutch Standard.
NEN. (2006b), *Application of mean hourly wind speed statistics for the Netherlands,* NPR 6097:2006 (in Dutch). Dutch Practice Guideline.
Richards, P.J. and Hoxey, R.P. (1993), "Appropriate boundary conditions for computational wind engineering models using the k-ε turbulence model", *J. Wind Eng. Ind. Aerodyn.*, **46&47**, 145-153.
Richards, P.J., Quinn, A.D. and Parker, S. (2002), "A 6 m cube in an atmospheric boundary layer flow. Part 2. Computational solutions", *Wind Struct.*, **5**(2-4), 177-192.
Richards, P.J., Mallison, G.D., McMillan, D. and Li, Y.F. (2002), "Pedestrian level wind speeds in downtown Auckland", *Wind Struct.*, **5**(2-4), 151-164.
Shih, T.H., Liou, W.W., Shabbir, A. and Zhu, J. (1995), "A new k-ε eddy-viscosity model for high Reynolds number turbulent flows – model development and validation". *Computers and Fluids*, **24**(3), 227-238.
Simiu, E. and Scanlan, R.H. (1986), *Wind effects on structures. An introduction to wind engineering. Second Edition*, John Wiley and Sons, New York.
Stathopoulos, T. and Storms, R. (1986), "Wind environmental conditions in passages between buildings", *J. Wind Eng. Ind. Aerodyn.*, **24**, 19-31.
Stathopoulos, T. (2002), "The numerical wind tunnel for industrial aerodynamics: Real or virtual in the new millennium?", *Wind Struct.*, **5**(2-4), 193-208.
Verkaik, J.W. (2006), *On wind and roughness over land*. PhD thesis, Wageningen Universiteit, Wageningen, The Netherlands.
Wieringa, J. (1992), "Updating the Davenport roughness classification", *J. Wind Eng. Ind. Aerodyn.*, **41-44**, 357-368.
Willemsen, E. and Wisse, J.A. (2002), "Accuracy of assessment of wind speed in the built environment", *J. Wind Eng. Ind. Aerodyn.*, **90**, 1183-1190.
Willemsen, E., and Wisse, J.A. (2007), "Design for wind comfort in The Netherlands: Procedures, criteria and open research issues", *J. Wind Eng. Ind. Aerodyn.*, in press. (doi:10.1016/j.jweia.2007.02.006).
Wiren, B.G. (1975), "A wind tunnel study of wind velocities in passages between and through buildings", *4th International Conference on Wind Effects on Buildings and Structures*, Heathrow.
Wise, A.F.E. (1970), "Wind effects due to groups of buildings", *Royal Society Symposium Architectural Aerodynamics*, London.
Wisse, J.A. and Willemsen, E. (2003), "Standardization of wind comfort evaluation in the Netherlands", *11th International Conference on Wind Engineering (11ICWE)*, Lubbock, Texas.
Wisse, J.A., Verkaik, J.W., and Willemsen, E. (2007), "Climatology aspects of a wind comfort code", *12th International Conference on Wind Engineering (12ICWE)*, Cairns, Australia.
Yang, W., Quan, Y., Jin, X., Tamura, Y. and Gu, M. (2007), "Influences of equilibrium atmosphere boundary layer and turbulence parameters on wind load distributions of low-rise buildings", *J. Wind Eng. Ind. Aerodyn.*, Accepted for publication.
Yoshie, R., Mochida, A., Tominaga, Y., Kataoka, H., Harimoto, K., Nozu, T. and Shirasawa, T. (2007), "Cooperative project for CFD prediction of pedestrian wind environment in the Architectural Institute of Japan", *J. Wind Eng. Ind. Aerodyn.*, 95(9-11): 1551-1578.

**Nomenclature**

| | |
|---|---|
| $C_s$ | roughness constant (dimensionless) |
| $C_\mu$ | constant for turbulent kinetic energy profile, parameter in the realizable k-ε model (dimensionless) |
| *B, L, H* | building width, length, height (m) |
| $k$ | turbulent kinetic energy (m²/s²) |
| $k_S$ | physical roughness height (m) |
| $L_D$, $W_D$, $H_D$ | length (streamwise), width (lateral) and height of computational domain (m) |
| $P$ | threshold exceedance probability (for all wind directions) (% time) |

| | |
|---|---|
| $P_\theta$ | threshold exceedance probability for wind direction $\theta$ (% time) |
| $u^*$ | friction velocity (m/s) |
| $U$ | local mean wind speed (magnitude of the 3D velocity vector) (m/s) |
| $U_0$ | reference mean wind speed (m/s) |
| $U_{pot}$ | potential wind speed (m/s) |
| $U_{THR}$ | threshold value for the local wind speed $U$ (m/s) |
| $x, y, z$ | Cartesian co-ordinates (x: streamwise, y: height, z: lateral) (m) |
| $y_0$ | aerodynamic roughness length (m) |
| $y_P$ | distance from the centre point of the wall-adjacent cell to the wall (m) |
| $\varepsilon$ | turbulence dissipation rate ($m^2/s^3$) |
| $\kappa$ | von Karman constant (~0.42) (dimensionless) |
| $\theta$ | wind direction (clockwise from north, north = 0°) |
| $\gamma$ | total wind amplification factor (dimensionless) |

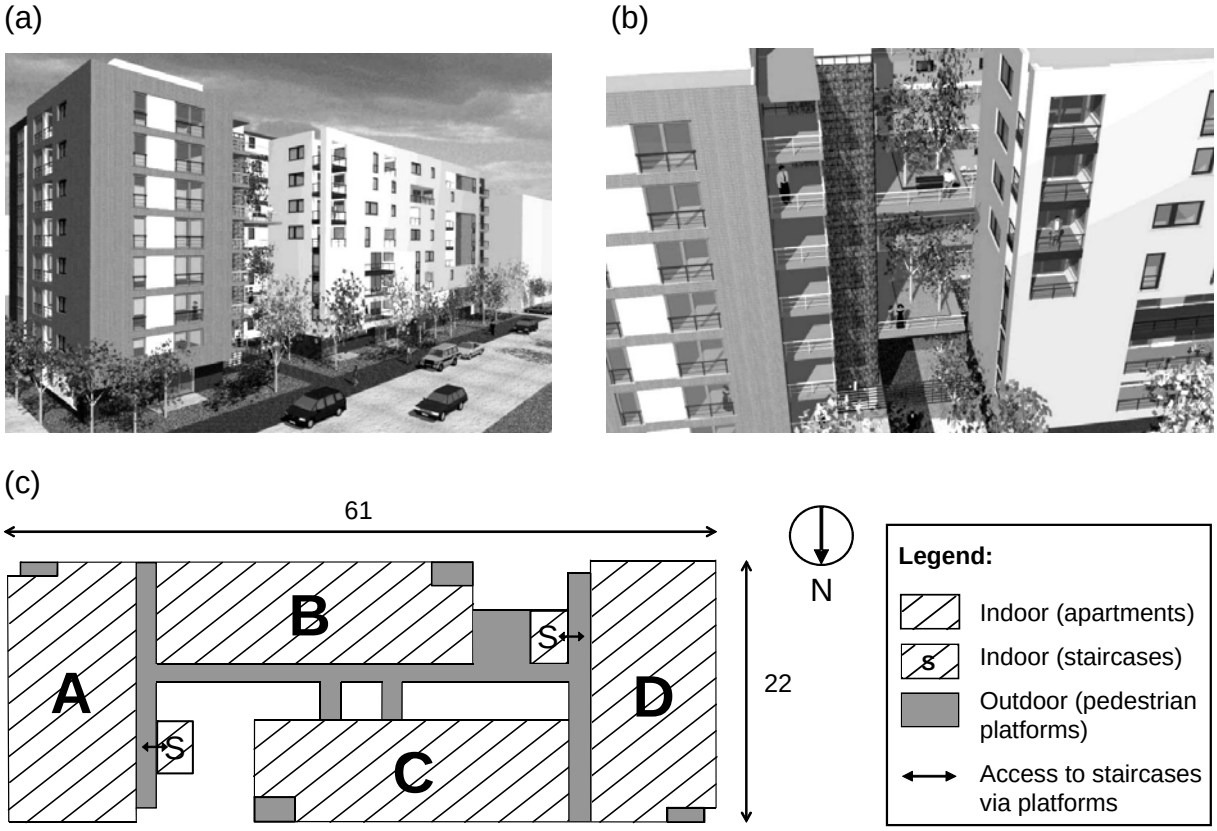


Fig. 1. Original design: (a) view from northeast; (b) view from north: detail of part of the outdoor pedestrian platforms; (c) schematic representation of intersection at the fifth floor.

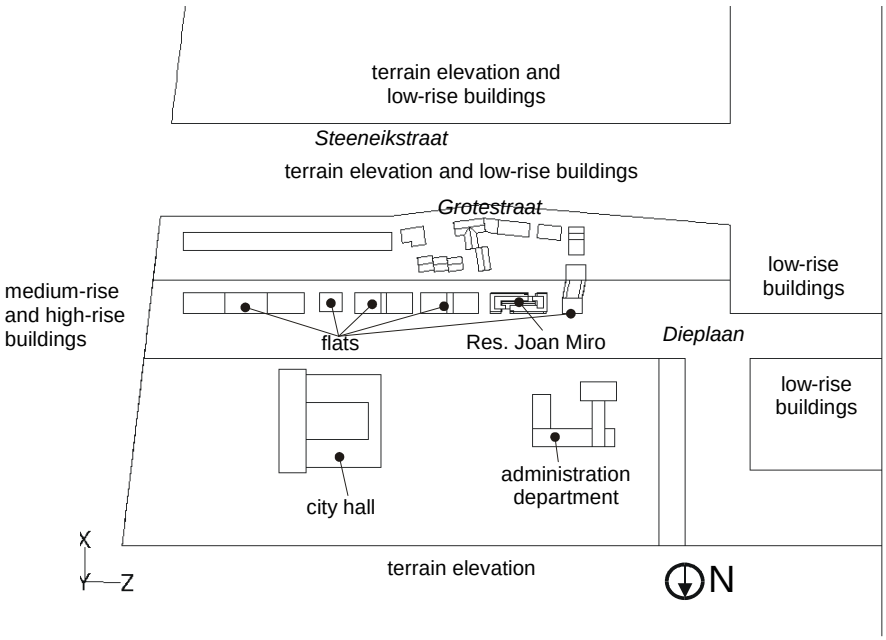


Fig. 2. Plan of apartment building (res. Joan Miro) and surrounding buildings in city centre. Street names are printed in italics.

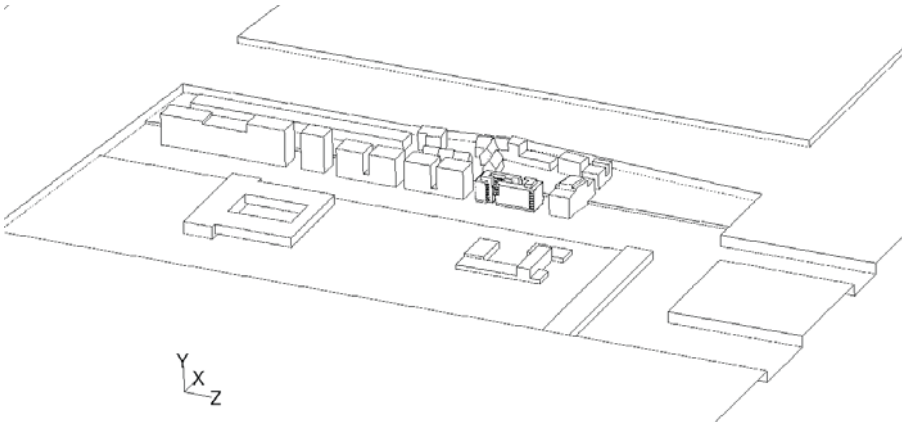


Fig. 3. Perspective view of apartment building, surrounding buildings and terrain elevation in city centre.

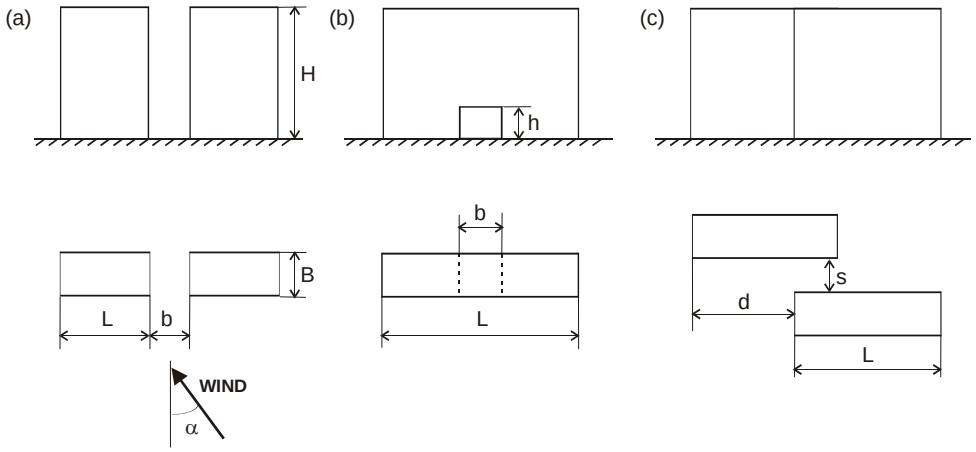


Fig. 4. Generic sub-configurations: (a) passage between two parallel buildings, placed side-by-side; (b) passage through a building; (c) passage between two parallel shifted buildings.

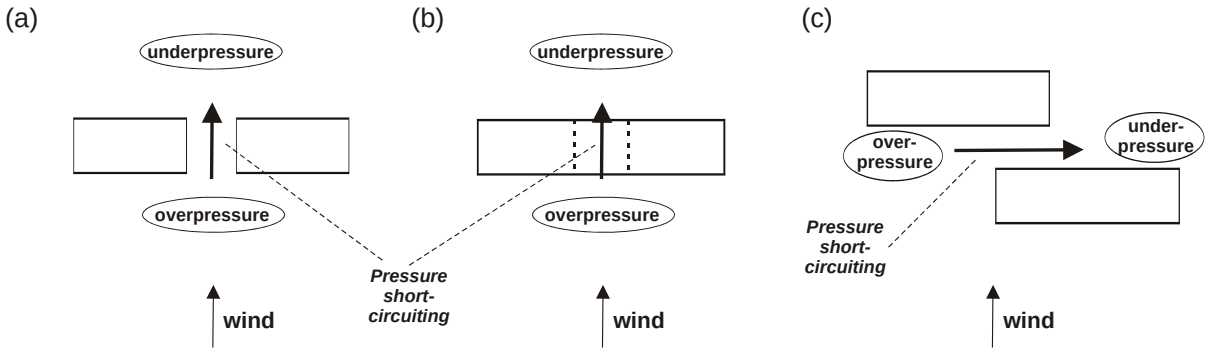


Fig. 5. Schematic representation (top view) of pressure short-circuiting for the three generic sub-configurations.

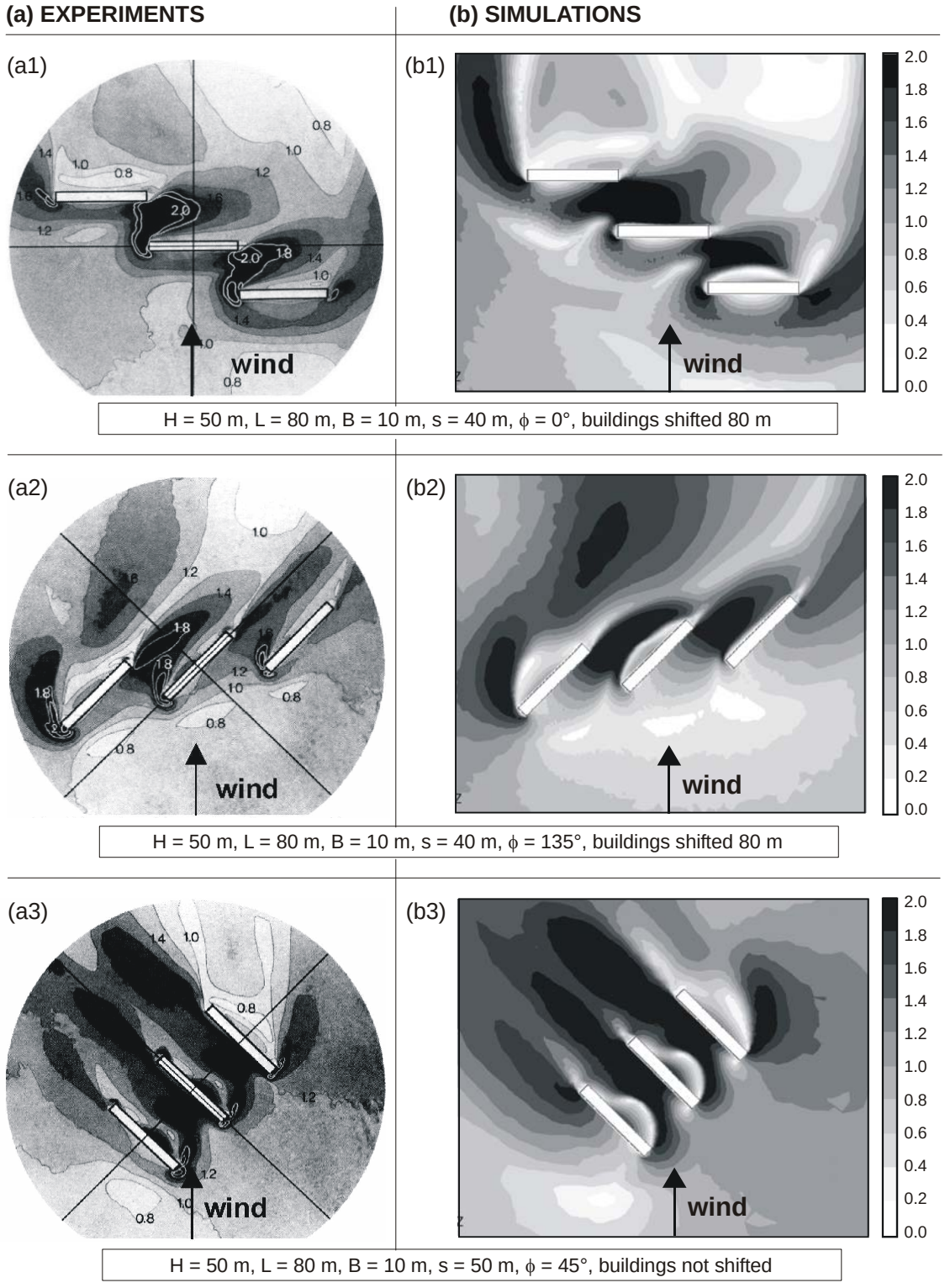


Fig. 6. Comparison of experimental and numerical results. (a) Top view of sand erosion contours on the wind tunnel turntable that provide a measure of the local wind amplification factor (Beranek 1982). White contour lines correspond to local amplification factors above 1.8 and 2.0. (b) CFD local wind amplification factors.

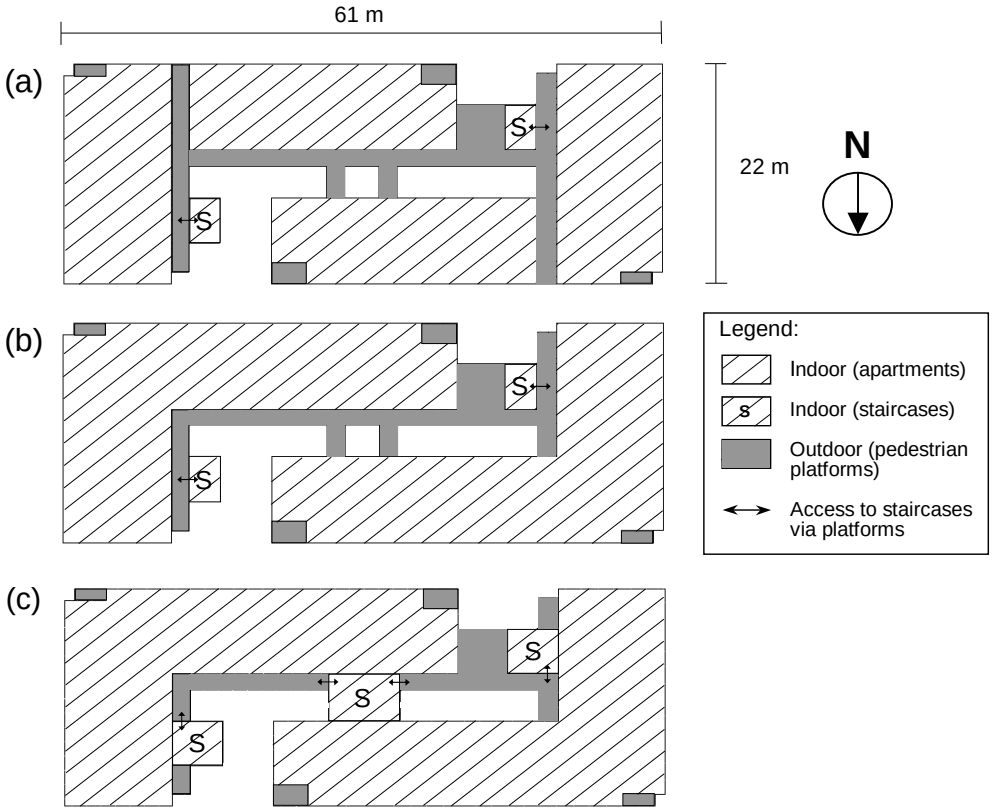


Fig. 7. Horizontal intersection at the fifth floor: (a) original design; (b) first design modification; (c) second design modification.

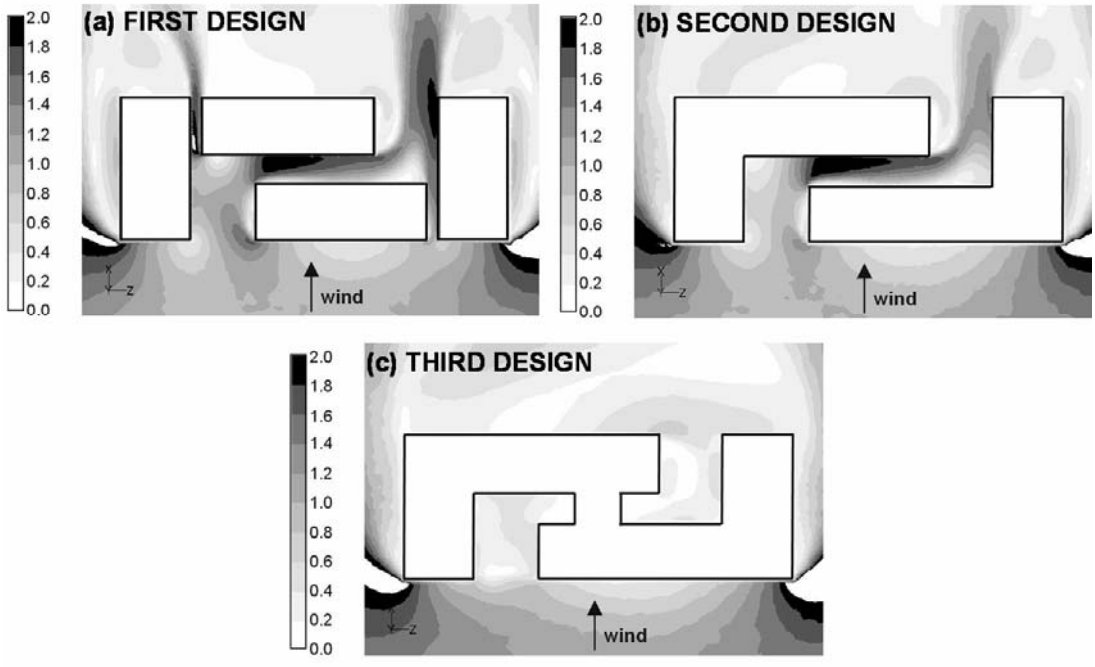


Fig. 8. Local wind amplification factors at 1.75 m height above ground-level for the three designs.

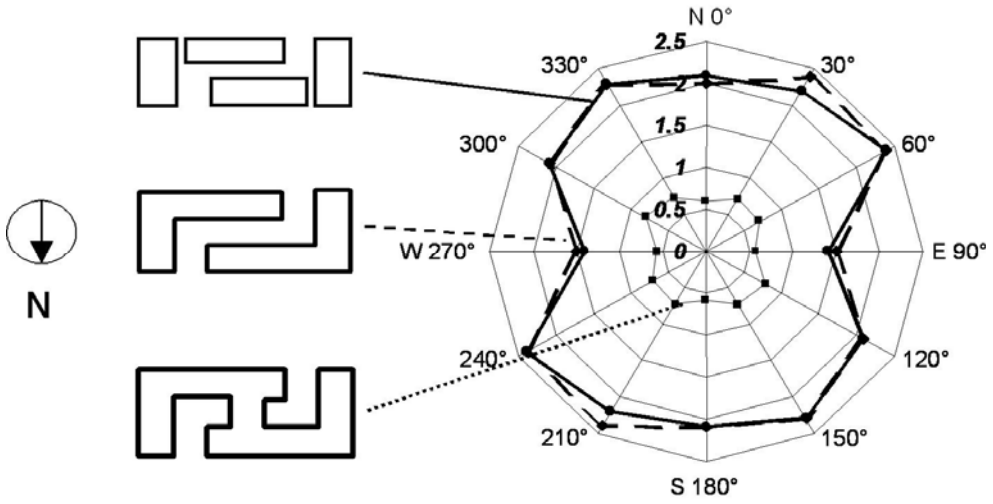


Fig. 9. Local wind amplification factor roses indicating the maximum values in the passage for the three designs and the 12 wind directions.

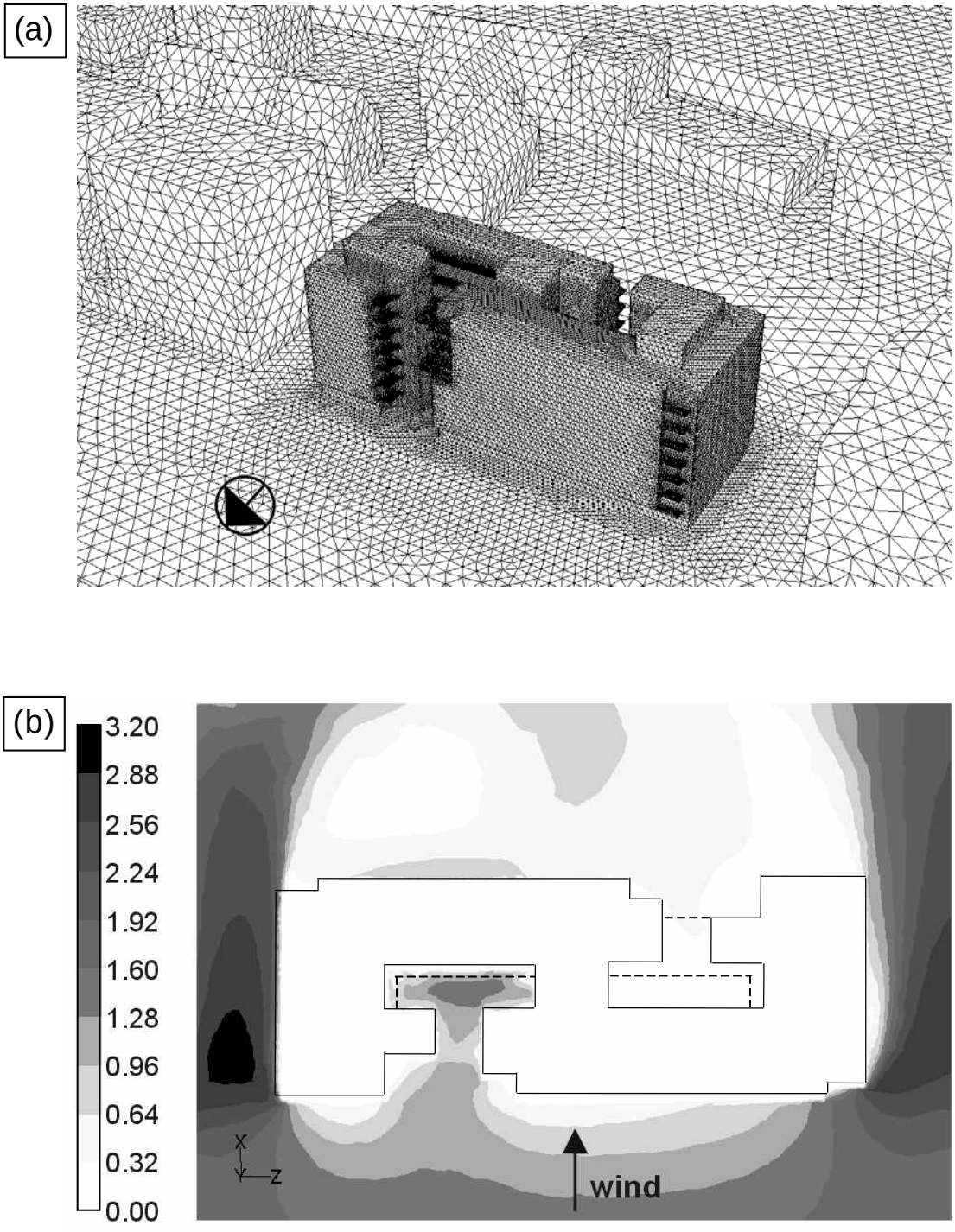


Fig. 10. (a) Grid on surface of apartment building and some surrounding buildings. (b) CFD local wind amplification factor in a horizontal plane at 1.75 m height above the fifth floor, for north wind. The edges of the outdoor pedestrian platforms at the fifth floor are indicated by dashed lines.

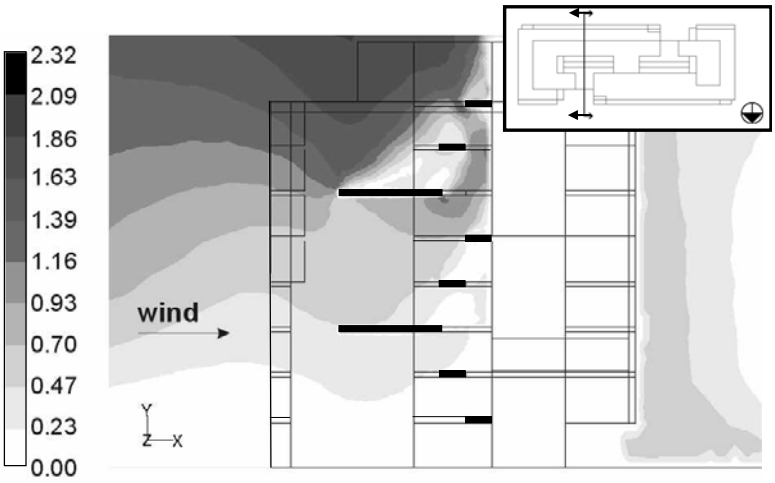


Fig. 11. Local wind amplification factor in a vertical plane cutting in north-south direction through the apartment building. The positions of the platforms in the north-facing cavity are indicated by black bars.

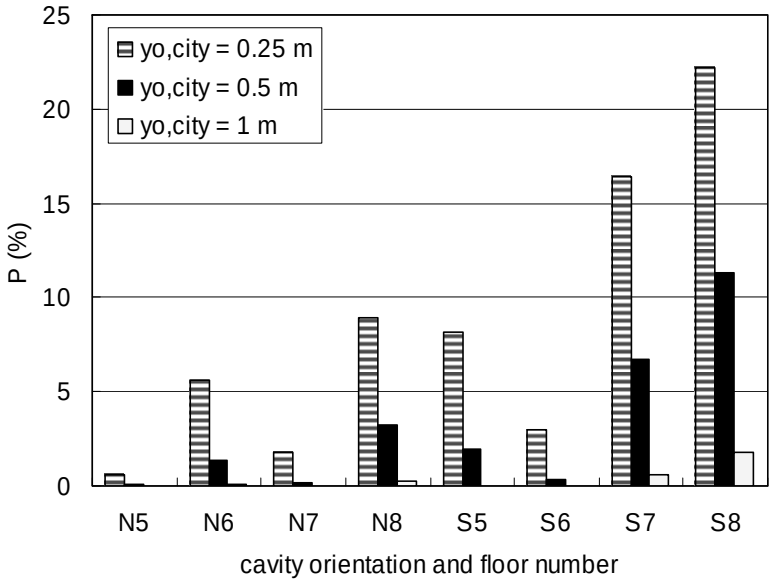


Fig. 12. Discomfort exceedance probabilities for the top four floors, for three consecutive roughness classes in the updated Davenport roughness classification.

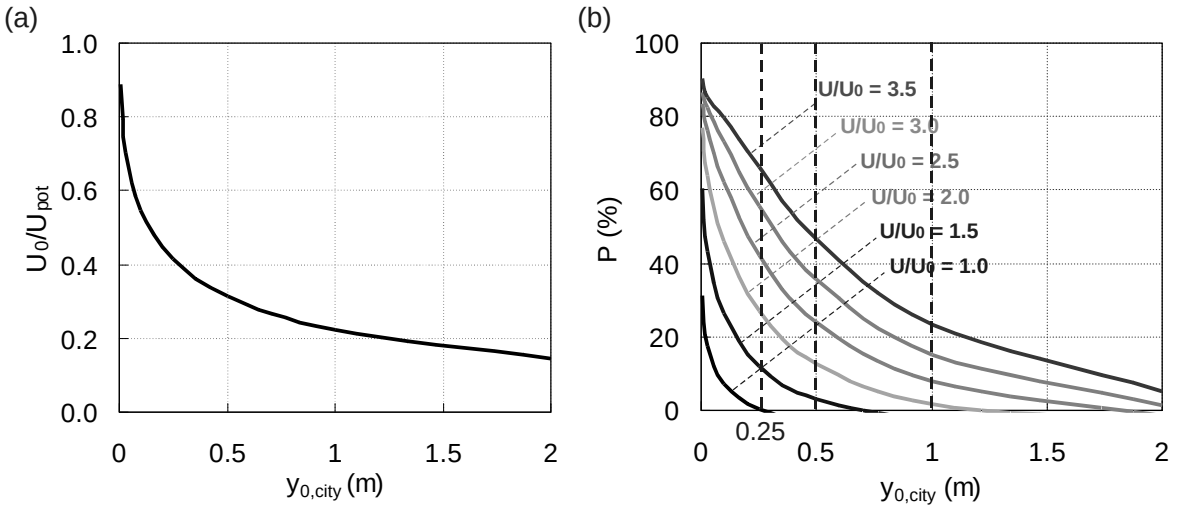


Fig. 13. (a) Variation of terrain related contribution $U_0/U_{pot}$ versus upstream aerodynamic roughness length $y_{0,city}$. (b) Variation of total discomfort probability P as a function of $y_{0,city}$, with the local wind amplification factor $U/U_0$ as a parameter.

Table 1: Criteria for wind comfort and danger according to NEN8100 (Willemsen and Wisse 2007).

| Wind comfort | | | | |
|---|---|---|---|---|
| $P(U_{THR} > 5$ m/s) (in % hours per year) | Grade | Activity | | |
| | | Traversing | Strolling | Sitting |
| < 2.5 | A | Good | Good | Good |
| 2.5 - 5.0 | B | Good | Good | Moderate |
| 5.0 - 10 | C | Good | Moderate | Poor |
| 10 - 20 | D | Moderate | Poor | Poor |
| > 20 | E | Poor | Poor | Poor |

| Wind danger | | |
|---|---|---|
| $P(U_{THR} > 15$ m/s) in % hours per year | Limited risk | 0.05 - 0.3 % hours per year |
| | Dangerous | > 0.3% hours per year |

## FIGURE CAPTIONS

Fig. 1. Original design: (a) view from northeast; (b) view from north: detail of part of the outdoor pedestrian platforms; (c) schematic representation of intersection at the fifth floor.

Fig. 2. Plan of apartment building (res. Joan Miro) and surrounding buildings in city centre. Street names are printed in italics.

Fig. 3. Perspective view of apartment building, surrounding buildings and terrain elevation in city centre.

Fig. 4. Generic sub-configurations: (a) passage between two parallel buildings, placed side-by-side; (b) passage through a building; (c) passage between two parallel shifted buildings.

Fig. 5. Schematic representation (top view) of pressure short-circuiting for the three generic sub-configurations.

Fig. 6. Comparison of experimental and numerical results. (a) Top view of sand erosion contours on the wind tunnel turntable that provide a measure of the local wind amplification factor (Beranek 1982). White contour lines correspond to local amplification factors above 1.8 and 2.0. (b) CFD local wind amplification factors.

Fig. 7. Horizontal intersection at the fifth floor: (a) original design; (b) first design modification; (c) second design modification.

Fig. 8. Local wind amplification factors at 1.75 m height above ground-level for the three designs.

Fig. 9. Local wind amplification factor roses indicating the maximum values in the passage for the three designs and the 12 wind directions.

Fig. 10. (a) Grid on surface of apartment building and some surrounding buildings. (b) CFD local wind amplification factor in a horizontal plane at 1.75 m height above the fifth floor, for north wind. The edges of the outdoor pedestrian platforms at the fifth floor are indicated by dashed lines.

Fig. 11. Local wind amplification factor in a vertical plane cutting in north-south direction through the apartment building. The positions of the platforms in the north-facing cavity are indicated by black bars.

Fig. 12. Discomfort exceedance probabilities for the top four floors, for three consecutive roughness classes in the updated Davenport roughness classification.

Fig. 13. (a) Variation of terrain related contribution $U_0/U_{pot}$ versus upstream aerodynamic roughness length $y_{0,city}$. (b) Variation of total discomfort probability P as a function of $y_{0,city}$, with the local wind amplification factor $U/U_0$ as a parameter.

## KEYWORDS

Numerical simulation; Computational Fluid Dynamics (CFD); Pedestrian wind comfort; Wind environment; Wind nuisance; Wind flow; Building passage; Validation; Wind tunnel measurements; Sand erosion